

# Intracellularly Degradable Hydrogen-Bonded Polymer Capsules

Kristian Kempe, Sher Leen Ng, Sylvia T. Gunawan, Ka Fung Noi, and Frank Caruso\*

The assembly of low-fouling polymer capsules with redox-responsive behavior and intracellular degradability is reported. Thiol-containing poly(2-ethyl-2-oxazoline) (PEtOxMA<sub>SH</sub>) brushes are synthesized by atom transfer radical polymerization (ATRP) of oligo(2-ethyl-2-oxazoline)methacrylate and glycidyl methacrylate (GMA) and subsequent ring-opening reaction of the GMA. Sequential deposition of PEtOxMA<sub>SH</sub>/poly(methacrylic acid) (PMA) multilayers onto silica (SiO<sub>2</sub>) particle templates and crosslinking through disulfide formation yield stable capsules after the removal of the SiO<sub>2</sub> templates by buffered hydrofluoric acid (HF). The redox-responsive nature of the disulfide crosslinking groups enables the degradation of these capsules under simulated intracellular conditions at pH 5.9 and 5 mM glutathione (GSH). Furthermore, capsule degradation is observed after incubation with dendritic (JAWS II) cells. Even at high capsule-to-cell ratios, PEtOxMA<sub>SH</sub> capsules show only negligible cytotoxicity. Quartz crystal microgravimetry (QCM) studies, using 100% human serum, reveal that films prepared from PEtOxMA<sub>SH</sub> exhibit low-fouling properties. The degradation and low-fouling properties are promising for application of PEtOxMA<sub>SH</sub> films/capsules for the delivery and triggered release of therapeutics.

## 1. Introduction

The design of smart polymeric carriers with tunable properties is of considerable interest for applications in drug delivery, catalysis, and microreactors.<sup>[1–4]</sup> Prerequisites for successful carriers are high biocompatibility, stability in the bloodstream, low-fouling characteristics, high encapsulation efficiencies as well as the ability to release encapsulated cargo on demand. The triggered release of payload has been the subject of extensive research during the last decade.<sup>[5,6]</sup> Various mechanisms and stimuli have been reported to induce the release of encapsulated cargo either by applying an external stimulus (e.g., temperature) or a biological trigger (e.g., pH, redox potential, or enzymatic change). Carriers that are responsive to biological changes are particularly desirable as they can, for example, innately respond upon sensing intracellular changes. Generally, biological triggers induce a change in the permeability of

the carrier systems and/or lead to their degradation.

To date, numerous techniques have been applied for the fabrication of delivery systems, including self-assembly and templated assembly.<sup>[7]</sup> Layer-by-layer (LbL)-templated polymer capsules, for example, have attracted increasing interest because of their potential for therapeutic delivery.<sup>[8,9]</sup> The versatility of the LbL process enables the fabrication of multilayered capsules with tailored properties.<sup>[10–12]</sup> In addition to the choice of the template, the assembly conditions, and the material interactions (e.g., electrostatics, hydrogen bonding, covalent interactions), the choice of the polymer system has a significant impact on the physical and chemical properties of the capsules.<sup>[7,13]</sup> A range of functional polymers has been used to assemble multilayer films and capsules through hydrogen bonding interactions,<sup>[12]</sup> including poly(methacrylic acid) (PMA) and poly(L-glutamic acid)

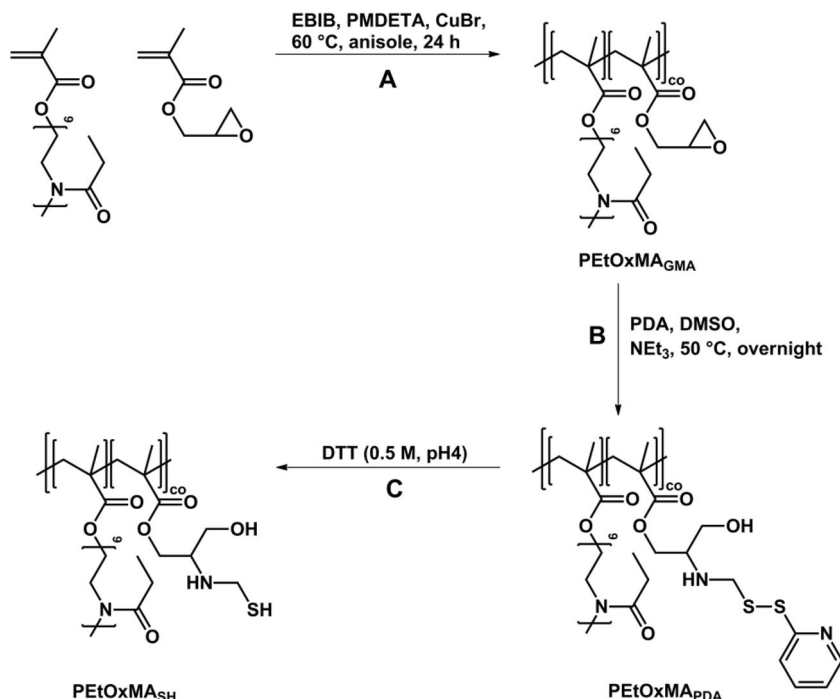
(PGA) as donors,<sup>[14]</sup> and poly(vinylpyrrolidone) (PVPON),<sup>[15,16]</sup> poly(ethylene glycol) (PEG)<sup>[17]</sup> and poly(2-oxazoline) as acceptors.<sup>[18,19]</sup> Hydrogen bonding assembled films are of particular interest because they can be designed to be responsive under biologically relevant conditions. Unlike electrostatically assembled films, they are not permanently charged, thus generally endowing them with lower fouling properties.<sup>[12]</sup>

Polymers functionalized with redox-responsive groups have been used to prepare carriers that are responsive to biological triggers.<sup>[20,21]</sup> This can be, for example, realized by using disulfide,<sup>[22,23]</sup> and diselenide chemistry,<sup>[24–26]</sup> which exploit differences between intra- and extra-cellular redox potentials. Disulfide-stabilized systems are cleavable within cells (reducing environment) due to the presence of glutathione (GSH) – an abundant intracellular thiol species.<sup>[27,28]</sup> We have reported the preparation of thiol-functionalized PMA (PMA<sub>SH</sub>), and its subsequent use to assemble single-component disulfide-stabilized capsules.<sup>[21,29]</sup> Furthermore, the incorporation of disulfide moieties into multilayered capsules was also accomplished by using disulfide-containing bisazide crosslinkers. This modular approach allowed redox-sensitive properties to be introduced to various alkyne-containing systems (e.g., poly(2-diisopropylaminoethyl methacrylate) (PDPA)<sub>Alk</sub>,<sup>[20]</sup> PVPON<sub>Alk</sub>,<sup>[15]</sup> or PEG<sub>Alk</sub><sup>[17]</sup> via copper-catalyzed cycloaddition. Degradation/disassembly of PMA<sub>SH</sub> as well as alkyne-functionalized polymer capsules

Dr. K. Kempe, Dr. S. L. Ng, S. T. Gunawan, K. F. Noi,  
Prof. F. Caruso  
Department of Chemical and Biomolecular Engineering  
The University of Melbourne  
Victoria 3010, Australia  
E-mail: fcaruso@unimelb.edu.au



DOI: 10.1002/adfm.201401397



**Scheme 1.** Synthesis of thiol-modified poly[oligo(2-ethyl-2-oxazoline methacrylate)-*stat*-glycidyl methacrylate] (PEtOxMA<sub>SH</sub>). A) Atom transfer radical polymerization (ATRP) of PEtOxMA and glycidyl methacrylate. B) Base-catalyzed ring-opening reaction using 2-(pyridylthio)-ethylamine (PDA). C) Prior to multilayer buildup: deprotection of thiol functionality using dithiothreitol (DTT).

was demonstrated under simulated intracellular conditions. Furthermore, extensive studies on PMA<sub>SH</sub> capsules revealed their potential to deliver and release various cargo in cells.<sup>[30,31]</sup> Disulfide crosslinked PDPA<sub>Alk</sub> capsules have been shown to undergo intracellular degradation into smaller fragments.<sup>[32]</sup> However, although both the PMA- and PDPA-based systems were shown to degrade in simulated intracellular and/or actual cellular environments, they exhibit fouling characteristics in their native capsule states (i.e., without post-functionalization).

Low-fouling materials/coatings decrease and/or resist non-specific protein adsorption,<sup>[33]</sup> which is a crucial property for advanced polymer carriers because they can allow efficient cargo delivery to a targeted site. To this end, we recently introduced poly(2-oxazoline)s (POxs) for the assembly of low-fouling polymer capsules.<sup>[34]</sup> It was shown that capsules prepared from brush-like POx exhibit promising low-fouling properties, as demonstrated by preliminary fouling tests with the model proteins bovine serum albumin (BSA) and lysozyme. In addition, the modularity of the cationic ring-opening polymerization (CROP) of functional 2-oxazolines provides access to highly functional polymer systems with tailor-made properties.<sup>[35–37]</sup> Linear and brush-like POxs with different crosslinkable functionalities have been synthesized and used for the fabrication of capsules.

Herein, we report the synthesis of brush-like poly(2-ethyl-2-oxazoline) (PEtOx) with pendant thiol moieties and the fabrication of redox-responsive LbL-assembled PEtOx capsules. These capsules are both intracellularly degradable and are comparatively lower fouling than counterpart PMA<sub>SH</sub> and PDPA<sub>Alk</sub> systems. The copolymer used in this study was obtained by

atom transfer radical polymerization (ATRP) of a PEtOx macromonomer and glycidyl methacrylate (GMA), and subsequent post-polymerization modification of the glycidyl groups with amine-containing disulfide linkers. This polymer system, which combines redox sensitivity with the low-fouling characteristics of PEtOx, was used for hydrogen bonding-driven LbL assembly on planar and particle supports. Stabilization of these multilayers was achieved by disulfide formation, which renders the respective capsules degradable under reducing conditions both in a simulated biological environment (GSH) and intracellularly.

## 2. Results and Discussion

### 2.1. Polymer Synthesis and Post-Polymerization Modification

To synthesize brush-like PEtOx systems with redox-sensitive disulfide groups, a three-step synthesis approach was chosen. Firstly, an oligo(2-ethyl-2-oxazoline methacrylate) (OEtOxMA) macromonomer was synthesized by CROP of 2-ethyl-2-oxazoline initiated with methyl tosylate and terminated with methacrylic acid.<sup>[38]</sup> Secondly, this macromonomer was copolymerized with glycidyl methacrylate (GMA) by ATRP to yield poly[oligo(2-ethyl-2-oxazoline methacrylate)-*stat*-glycidyl methacrylate] (PEtOxMA<sub>GMA</sub>). After purification, PEtOxMA<sub>GMA</sub> was modified with 2-(pyridylthio)-ethylamine (PDA) via ring-opening reaction of the glycidyl groups to introduce redox-sensitive disulfide moieties (PEtOxMA<sub>PDA</sub>). Treatment with dithiothreitol (DTT) prior to multilayer buildup afforded brush-like POx with free thiol groups, referred to as PEtOxMA<sub>SH</sub> (Scheme 1).

Using <sup>1</sup>H NMR, the degree of polymerization and the degree of functionalization were determined. For the synthesis of the OEtOxMA, full conversion of the 2-ethyl-2-oxazoline (EtOx) monomer was obtained, which corresponds to six EtOx units (Figure S1, Supporting Information). The copolymer obtained by copolymerization of OEtOxMA with GMA contained 15 mol% glycidyl groups, which were quantitatively consumed in the ring-opening reaction with PDA, as can be seen by the disappearance of the respective <sup>1</sup>H NMR signals (2.6–2.8 ppm, 4.2 ppm). The appearance of aromatic signals (7.0–8.5 ppm) proved the successful modification with pyridyl containing disulfide groups (Figure 1). Size exclusion chromatography (SEC) measurements revealed the synthesis of well-defined copolymers with polydispersity (*D*) values < 1.35.

### 2.2. Multilayer Assembly on Planar and Particle Supports

The assembly of PEtOxMA<sub>SH</sub> and PMA multilayer films via hydrogen bonding was monitored on planar and particle supports using quartz crystal microgravimetry (QCM) and flow

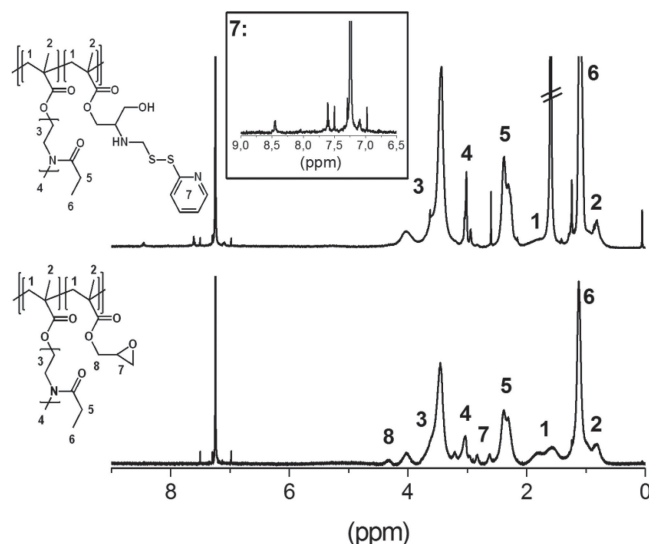


**Figure 1.**  $^1\text{H}$  NMR spectra of poly[oligo(2-ethyl-2-oxazoline methacrylate)-*stat*-glycidyl methacrylate] (PEToxMA<sub>CMA</sub>) synthesized by ATRP (bottom), which was modified subsequently with 2-(pyridylthio)-ethylamine (PDA) in a base-catalyzed ring-opening reaction (top).

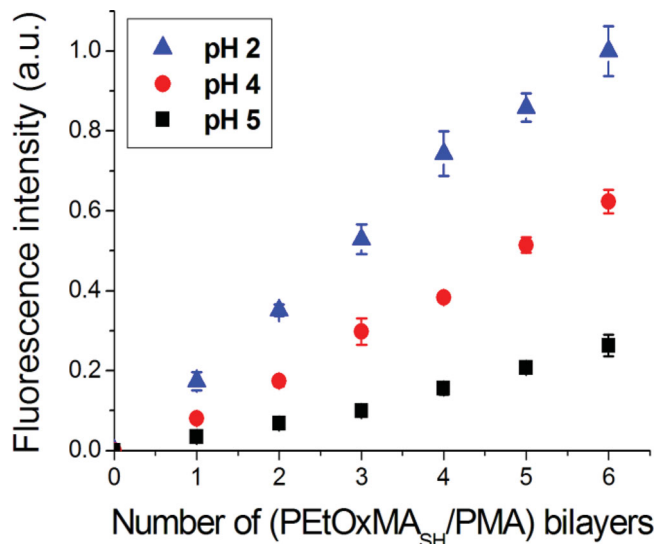
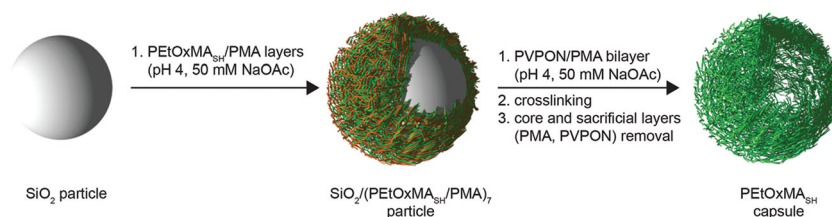


**Figure 2.** LbL film assembly of PEToxMA<sub>SH</sub>/PMA bilayers (50 mM NaOAc) at different pH on particle supports (SiO<sub>2</sub>, 2.59  $\mu\text{m}$  diameter), as monitored by flow cytometry. PMA was prelabeled with AF488<sub>cad</sub>. Measurements were taken after each PMA layer was deposited.

cytometry, respectively. For both studies, PEToxMA<sub>PDA</sub> was treated with DTT (0.5 M) prior to layer buildup to deprotect the thiol groups. Polymer solutions were prepared in 1 g L<sup>-1</sup>, 50 mM sodium acetate buffer (NaOAc) at pH 4. The formation of PEToxMA<sub>SH</sub>/PMA hydrogen-bonded multilayers was first examined by QCM. To this end, gold substrates were coated with an initial layer of polyethylene imine (PEI) (1 g L<sup>-1</sup> in 0.5 M NaCl). The film was washed into 50 mM NaOAc and PMA (1 g L<sup>-1</sup> in 50 mM NaOAc) was allowed to adsorb for 15 min. After washing the film in NaOAc buffer, PEToxMA<sub>SH</sub> (1 g L<sup>-1</sup> in 50 mM NaOAc) was adsorbed for 20 min followed by another washing step. This procedure was repeated until 7 bilayers were obtained. Layer buildup at pH 4 followed a linear trend: the QCM frequency decreased with an increasing number of layers (Figure S2, Supporting Information). Studies on particle supports were performed on monodisperse SiO<sub>2</sub> particles (2.59  $\mu\text{m}$  in diameter) at pH 2, 4 and 5 (50 mM NaOAc). Prior to the first layer, the SiO<sub>2</sub> particles were washed into the respective buffer. Subsequently, the particles were incubated in PEToxMA<sub>SH</sub> (1 g L<sup>-1</sup> in 50 mM NaOAc) and PMA (1 g L<sup>-1</sup> in 50 mM NaOAc), respectively. The polymers were allowed to adsorb for 12 min with constant shaking before washing them via three centrifugation/redispersion cycles. In order to monitor and compare the buildup, PMA was prelabeled with Alexa Fluor 488-cadaverine (AF488<sub>cad</sub>) and the fluorescence intensity of the particles was measured by flow cytometry after the deposition of each bilayer. Regular and linear buildup was observed for all pH values (Figure 2). Due to the greater degree of protonation of the PMA ( $\text{pK}_a \approx 6$ ), hydrogen bonding is more pronounced at lower pH values, resulting in a higher fluorescence intensity, which corresponds to higher mass deposition.

For the fabrication of hollow PEToxMA<sub>SH</sub> capsules, polymer solutions (1 g L<sup>-1</sup>) at pH 4 (50 mM NaOAc) were used. Seven PEToxMA<sub>SH</sub>/PMA bilayers were deposited onto SiO<sub>2</sub> particle templates (2.59  $\mu\text{m}$  in diameter). In addition, two non-functionalized sacrificial PVPON/PMA layers were deposited as capping layers (Scheme 2) to minimize interparticle crosslinking and thus aggregation. To crosslink the thiol moieties of the PEToxMA<sub>SH</sub> layers within the multilayer films, the core-shell particles were stirred at elevated temperatures overnight. After removal of the SiO<sub>2</sub> core by hydrofluoric acid (HF) treatment and the sacrificial PMA and PVPON layers by washing into PBS (pH 7.4), the capsules formed were labeled with AF488-maleimide (AF488<sub>mal</sub>). Analysis of the capsules using fluorescence microscopy revealed swelling of the capsules (Figure 3a). A decrease in pH to 5.9 had only a marginal influence on the capsule size (Figure 3b). Representative air-dried TEM images of PEToxMA<sub>SH</sub> capsules at pH 7.4 and pH 5.9 are shown in Figure S3, Supporting Information. Furthermore, the capsules were analyzed using AFM (Figure S4, Supporting Information), which showed spherical structures with folds and creases, which are typical for polymer capsules prepared by the LbL technique.



**Scheme 2.** Preparation of disulfide-stabilized PEToxMA<sub>SH</sub> capsules via hydrogen-bonded LbL assembly of PEToxMA<sub>SH</sub> and PMA.

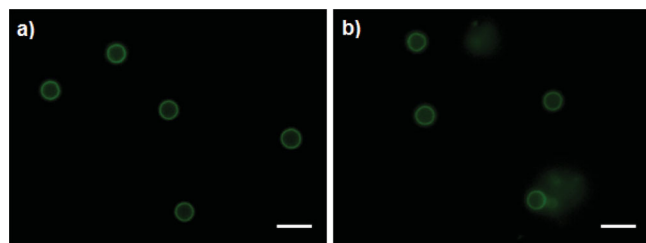


**Figure 3.** Fluorescence microscopy images of PEToxMA<sub>SH</sub> capsules at a) pH 7.4 and b) pH 5.9 (PBS, 50 mM). Multilayer assembly was performed on sacrificial SiO<sub>2</sub> particles (2.59 μm diameter) at pH 4 (NaOAc, 50 mM). The core-shell particle were treated with HF to remove the core and washed into PBS to remove sacrificial PMA and PVPON. The capsules were labeled with AF488<sub>mal</sub>. Scale bar = 5 μm.

### 2.3. Degradation Studies on Planar Films and Capsules

First, the degradability of PEToxMA<sub>SH</sub> multilayer films was studied using QCM (**Figure 4**). To this end, four PEToxMA<sub>SH</sub>/PMA bilayers were adsorbed onto a SiO<sub>2</sub> QCM crystal coated with PEI and PMA<sub>SH</sub>. Subsequently, the films were stabilized by incubation with chloramine T, which oxidizes the free thiol moieties, inducing the formation of disulfide bonds. An increase in frequency was observed after a PBS/NaOAc washing cycle, reflecting the loss of the sacrificial PMA layers. Exposure of the films to DTT enabled the reduction of the disulfide bonds and led to disassembly of the PEToxMA<sub>SH</sub> films. This is supported by the significant increase in the frequency observed, which is an indication of polymer loss.

The degradation of PEToxMA<sub>SH</sub> capsules was studied under simulated intracellular conditions. The incorporation of redox-responsive groups into the carriers allows us to exploit the redox potential differences within biological systems for degradation and/or triggered release of cargo in the intracellular environment. The reducing environment inside cells triggers the disintegration of disulfide stabilized systems. The

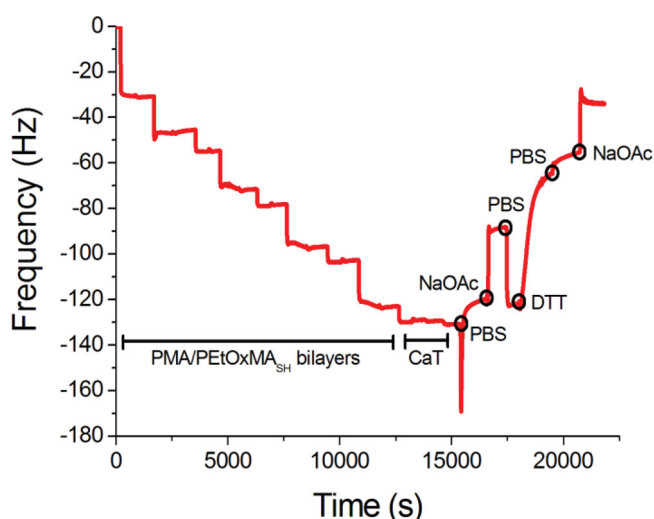


**Figure 4.** Multilayer film buildup via LbL assembly at pH 5, film stabilization with chloramine T (CaT), and disassembly of the film with dithiothreitol (DTT), as monitored in situ by QCM.

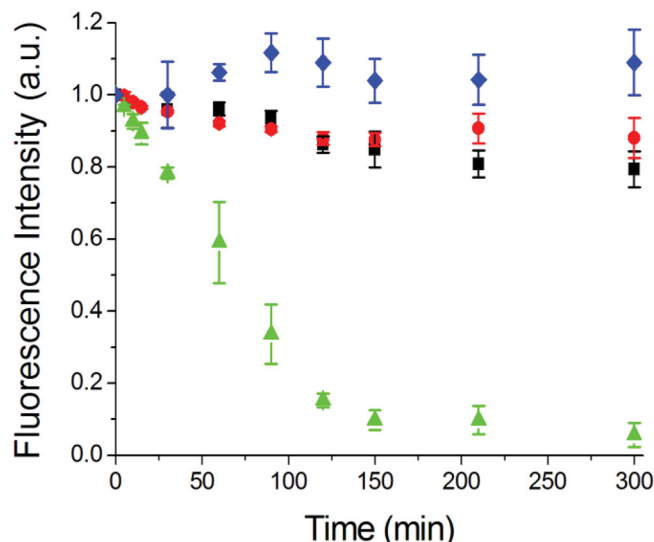


**Figure 5.** Degradation profiles of (PEToxMA<sub>SH</sub>)<sub>7</sub> capsules, as monitored by flow cytometry: PBS, pH 7.4 (black squares), pH 5.9 (red circles), and 5 mM GSH at pH 5.9 (green triangles). As a control, nondegradable (stabilized with bismaleimide crosslinker) capsules were incubated in 5 mM GSH, pH 5.9 (blue diamonds). Experiments were performed in triplicates.

average concentration of GSH within cells is reported to vary between 0.5 and 10 mM.<sup>[22,23]</sup> Cellular uptake of particular carriers typically occurs via endocytic mechanisms.<sup>[39]</sup> Therefore, to simulate these conditions, we incubated the capsules in PBS (at endosomal pH 5.9) at 37 °C with 5 mM GSH and monitored the fluorescence intensity of the AF488<sub>mal</sub>-labeled capsules over time using flow cytometry (**Figure 5**). A steady decrease in the fluorescence intensity over time was observed, indicative of degradation of the capsules. In contrast, no significant decrease in fluorescence intensity of the capsules was observed for the control conditions (i.e., upon incubation of the capsules in PBS (pH 5.9 and 7.4) without GSH), demonstrating the necessity of a reducing environment for destabilization of the capsules. To study the influence of the disulfide crosslinks, capsules stabilized by Michael-addition reaction between the free thiol groups in the PEToxMA<sub>SH</sub> layers and bismaleimide crosslinkers were prepared, rendering the capsules resistant against reducing agents, such as GSH. Incubation of these capsules in PBS (pH 5.9) at 37 °C with 5 mM GSH caused virtually no decrease in the fluorescence intensity, as monitored by flow cytometry, and thus suggested that these capsules remained stable under simulated intracellular reducing conditions.

### 2.4. Cell Studies

To study the potential of a carrier system for drug delivery applications, its cellular interactions need to be examined. Here, we used JAWS II cells, an immortalized immature dendritic cell (DC) line harvested from mouse bone marrow. DCs are extensively studied in particular because of their critical roles in activating both T and B cells during an immune response and as targeted cell lines for immunotherapy against cancers and various infectious diseases. First, the cytotoxicity of the capsules



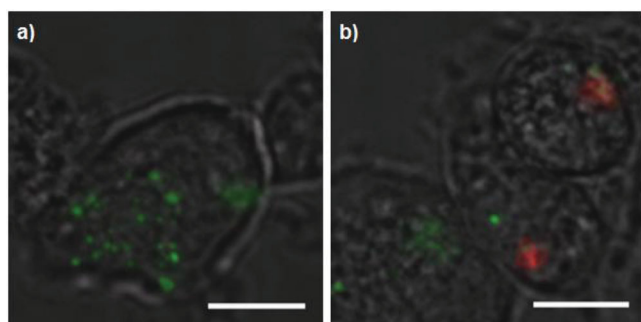


**Figure 6.** Magnified deconvolution optical microscopy images (with maximum intensity projection) of JAWS II cells incubated for 24 h with a) degradable PEToxMA<sub>SH</sub> capsules (green), and b) degradable (green) and nondegradable (red) PEToxMA<sub>SH</sub> capsules. Scale bar = 10 μm.

against JAWS II cells was investigated using an XTT assay (Figure S5, Supporting Information). The results suggested that even at high capsule-to-cell ratios, negligible cytotoxicity was observed. Furthermore, cell association/internalization kinetics of the PEToxMA<sub>SH</sub> capsules with the cells at 37 °C demonstrated cellular association/uptake within a few hours (Figure S6, Supporting Information). To examine the intracellular degradation of the PEToxMA<sub>SH</sub> capsules, AF488<sub>mal</sub>-labeled capsules were incubated with JAWS II cells (at a capsule-to-cell ratio of approximately 10:1) at 37 °C over 24 h and investigated with deconvolution optical microscopy (Figure 6 and Figure S7, Supporting Information). Capsule degradation was observed, as can be seen by the formation of fluorescent fragments from intact capsules (Figure 6a). To prove that the disintegration of the capsules is caused by the disruption of the disulfide bonds within the PEToxMA<sub>SH</sub> capsule wall, JAWS II cells were incubated with AF488<sub>mal</sub>-labeled degradable and AF647<sub>mal</sub>-labeled nondegradable (bismaleimide-stabilized) capsules. In contrast to the degradable capsules, the nondegradable capsules only showed slight structural deformation, without the formation of fluorescent fragments inside the cells (Figure 6b). This result is in accordance with the degradation profiles obtained under simulated intracellular conditions (Figure 5), highlighting the role of the disulfide bonds for intracellular degradation.

## 2.5. Fouling Studies with Human Serum

Extended blood circulation times are of high importance for potential carrier systems to increase their bioavailability for the efficient delivery of cargo to specific sites of action. To achieve this, carriers and surfaces are typically composed of or modified with materials that render the systems low-fouling to avoid rapid recognition, and hence clearance from the body.<sup>[40,41]</sup> Recently, we demonstrated the potential of PETox as a low-fouling material for the fabrication of hydrogen-bonded LbL films using two representative proteins, namely BSA and lysozyme.<sup>[34]</sup> Here, we extend this study by using full human blood serum. To evaluate the fouling characteristics of PEToxMA<sub>SH</sub> multilayered films, hydrogen-bonded PEToxMA<sub>SH</sub>/PMA films were assembled, stabilized, and washed into PBS, as monitored by QCM. For comparison, PETox<sub>Alk</sub>, PMA<sub>SH</sub> and PDPA<sub>Alk</sub> films were also assembled. (See Figure S8, Supporting

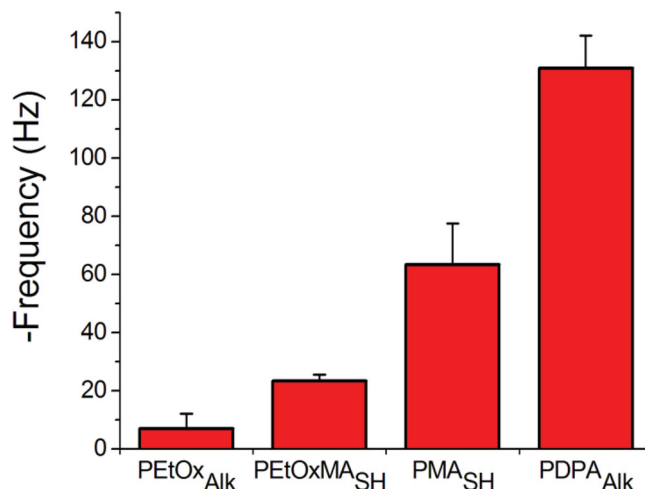


**Figure 7.** Adsorption of human serum proteins on PETox<sub>Alk</sub>, PEToxMA<sub>SH</sub>, PMA<sub>SH</sub>, and PDPA<sub>Alk</sub> films on planar supports, as monitored by QCM.

Information, for the chemical structures of PETox<sub>Alk</sub>, PMA<sub>SH</sub> and PDPA<sub>Alk</sub>.) All films were incubated in 100% human blood serum for 45 min and subsequently washed in PBS to remove any unbound serum proteins. For all films, the dissipation-to-frequency ratios of the films were low ( $< 1 \times 10^{-6}$  per 10 Hz).<sup>[42]</sup> Thus, the frequency changes observed correspond to the mass of protein adsorbed and was used as a representative measure for the fouling properties of the respective films (Figure 7). PEToxMA<sub>SH</sub> films ( $\Delta F = 23 \pm 2$  Hz) showed slightly higher adsorption of serum proteins than previously reported for low-fouling PVPON films ( $\Delta F = 18 \pm 3$  Hz).<sup>[17]</sup> In contrast, the frequency decreases for films made of PMA<sub>SH</sub> and PDPA<sub>Alk</sub>, were evaluated to be  $64 \pm 14$  Hz and  $131 \pm 11$  Hz, respectively. Thus, the direct comparison of PMA<sub>SH</sub> and PEToxMA<sub>SH</sub> systems, which are both prepared from polymers with pendant thiol groups, demonstrates a three-fold reduction in fouling. Furthermore, it is noted that a significant improvement in fouling was observed in comparison to the intracellularly degradable PDPA<sub>Alk</sub> LbL system. Both observations highlight the beneficial properties of the comparatively lower fouling PEToxMA<sub>SH</sub> system. In addition, the higher serum protein adsorption for the PEToxMA<sub>SH</sub> films (over PETox<sub>Alk</sub> films) is attributed to the free, non-crosslinked thiol groups available within the films, which increase film interactions with the serum proteins. PETox<sub>Alk</sub> films, free from thiol pendants, stabilized with a non-degradable bisazide linker showed a significantly lower frequency change after incubation with human blood serum.

## 3. Conclusion

The fabrication of redox-responsive, intracellularly degradable poly(2-ethyl-2-oxazoline) (PETox) capsules is presented. Brush-like thiol-containing PETox was obtained in a three-step synthesis, which involved the synthesis of a PETox-based macromonomer by atom transfer radical polymerization (ATRP) with glycidyl methacrylate (GMA), and post-polymerization modification with 2-(pyridylthio)-ethylamine (PDA). Multilayer films were prepared on planar and particle supports. The thiol/

disulfide exchange reaction was employed for stabilization of the polymer films, and also endowed the films with redox-responsive properties. Disassembly of the polymer capsules was demonstrated under simulated (reducing) intracellular conditions, that is, at pH 5.9 and 5 mM GSH. Intracellular degradation was observed upon incubation of the capsules in JAWS II cells. Furthermore, incubation studies on planar films in 100% human serum revealed protein adsorption similar in magnitude to other low-fouling (e.g., PEG-based) LbL polymer films,<sup>[17]</sup> and demonstrated enhanced properties over charged LbL polymer films. The intracellular degradation of the PEtOx capsules in combination with the low-fouling properties makes them of interest for bioapplications, including the delivery and release of therapeutics.

## 4. Experimental Section

**Materials and Instrumentation:** Silica particles were purchased from MicroParticles GmbH (Germany) as a 5 wt% suspension and were used as received. Poly(methacrylic acid, sodium salt) (PMA, 30 wt%),  $M_w$  15 kDa, was purchased from Polysciences (USA). Poly(*N*-vinylpyrrolidone) (PVPON),  $M_w$  10 kDa, 2-ethyl-2-oxazoline, methyl tosylate, and triethylamine were purchased from Sigma-Aldrich, distilled to dryness and stored under argon. Acetonitrile, anisole, dithiothreitol (DTT), glutathione (GSH), chloramine-T hydrate (CaT), glycidyl methacrylate (GMA), ethyl  $\alpha$ -bromoisobutyrate (EBIB), *N,N,N',N',N''*-pentamethyldiethylenetriamine (PMDETA), copper(I) bromide (CuBr), triethylamine, dimethylsulfoxide (DMSO), phosphate buffered saline (PBS) tablets, and buffering salts were purchased from Sigma-Aldrich and used as received. Alexa Fluor dyes, XTT ((2,3-Bis-(2-Methoxy-4-Nitro-5-Sulphophenyl)-2H-Tetrazolium-5-Carboxanilide), PMS (phenazine methosulfate), Recombinant Mouse Granulocyte Macrophage Colony-Stimulating Factor (GM-CSF) recombinant mouse protein, and MEM alpha were obtained from Life Technologies, Inc. Fetal bovine serum (FBS) was purchased from JRH Biosciences. High-purity water with a resistivity greater than 18 M $\Omega$  cm was obtained from an in-line Millipore RHO/Origin water purification system (Milli-Q water). 2-(pyridylthio)-ethylamine (PDA) was synthesized according to the literature.<sup>[43]</sup> Fluorescence microscopy measurements were performed with an inverted Olympus IX71 microscope equipped with a DIC slider (U-DICT, Olympus) with a 60 $\times$  objective lens (Olympus UPLFL20/0.5 N.A., W.D. 1.6) and used to visualize the capsules. A CCD camera (Cool SNAP *fx*, Photometrics, Tucson, AZ) was mounted on the left hand port of the microscope. Fluorescence images were illuminated with an Hg arc lamp using a UF1032 filter cube. TEM images were taken with a Philips CM120 BioTWIN microscope, operated at 120 kV. The sample solution (2  $\mu$ L) was placed onto a carbon-coated Formvar film mounted on 300-mesh UV-treated copper (ProSciTech, Australia) and allowed to air-dry overnight. AFM measurements were carried out on a cypher (Asylum Research AFM). The sample solution (10  $\mu$ L) was placed onto mica and air-dried overnight. Tapping mode cantilevers (BudgetSensors, Tap-300G, resonance frequency; 300 kHz, force constant; 40 N m<sup>-1</sup>) were used. A Partec CyFlow Space (Partec GmbH, Germany) flow cytometer, using an excitation wavelength of 488 nm, was used for all flow cytometry experiments. Data analysis was performed with Partec CyFlowMax software or FlowJo analysis software to obtain the fluorescence intensities of the samples. The in vitro capsule degradation study was performed with a deconvolution microscope (DeltaVision, Applied Precision, 60 $\times$  1.42 NA oil objective) to visualize the intracellular degradation of the capsules. The filter sets used were FITC and CY5 to observe the AF488-labeled degradable and AF647 nondegradable capsules inside the cells, respectively. The images were taken after 24 h sample incubation with JAWS II cells (with an approximately 10:1 capsule-to-cell ratio), deconvolved, and then analyzed using Imaris

(Bitplane) software to obtain the 3D images with maximum intensity projection. The cell viability assay was analyzed by measuring the sample absorbance at 450 nm. The absorbance at 450 nm was then measured using an Infinite M200 microplate reader (Tecan, Switzerland).

**Oligo(2-ethyl-2-oxazoline methacrylate) (OEtOxMA):** The OEtOxMA macromonomer was synthesized according to a literature procedure.<sup>[44]</sup> A solution of methyl tosylate (l; 1.2 g; 6.44 mmol) and 2-ethyl-2-oxazoline (EtOx; 4 g; 40 mmol) was prepared in acetonitrile (3.8 g; 92.6 mmol). The total monomer concentration was adjusted to 4 M with a [EtOx]:[l] ratio of 6:1. The sealed vial was heated to 85 °C in an oil bath for 60 min. After cooling, methacrylic acid (0.8 mL; 9.66 mmol) and triethylamine (1.8 mL; 12.89 mmol) were added to the polymerization mixture and stirring was continued overnight at 50 °C. Subsequently, the polymer was purified by washing with sodium bicarbonate and brine. The combined organic phases were dried over magnesium sulfate, filtered and the solvent was removed under reduced pressure. OEtOxMA was obtained after drying the polymer for 2 days in high vacuo. <sup>1</sup>H NMR analysis demonstrated the quantitative conversion of the monomer and quantitative functionalization with methacrylic acid. SEC (THF, PS standard):  $M_n$  = 1 100 g mol<sup>-1</sup>,  $\delta$  = 1.11.

**Poly(oligo(2-ethyl-2-oxazoline methacrylate)-stat-glycidyl methacrylate) (PEtOxMA<sub>GMA</sub>):** PEtOxMA was prepared by atom transfer radical polymerization (ATRP). OEtOxMA (1 g; 1.54 mmol) and PMDETA (19.9 mg; 0.11 mmol) were dissolved in anisole (3.5 mL) and degassed for 30 min. In parallel, GMA (36.2 mg; 0.25 mmol) and EBIB (3.3 mg; 0.017 mmol) were dissolved in anisole (1 mL) and CuBr (15.5 mg; 0.11 mmol) was added. The suspension was degassed for 30 min. The total monomer concentration was adjusted to 0.4 M with a [OEtOxMA]:[GMA]:[EBIB] ratio of 90:15:1. The OEtOxMA solution was added to the CuBr suspension and then reacted at 60 °C for 24 h. After cooling to room temperature, the polymer was precipitated in ice-cold diethyl ether, re-dissolved in dichloromethane and passed through a neutral alumina column. Subsequently, the polymer was recovered by precipitation in ice-cold diethyl ether. <sup>1</sup>H NMR revealed 60% and 70% conversion for OEtOxMA and GMA, respectively. <sup>1</sup>H NMR (400 MHz, CDCl<sub>3</sub>,  $\delta$ ): 4.47–4.21 (COO-CH<sub>2</sub> GMA), 4.18–3.2 (N-CH<sub>2</sub> POxMA), 3.15–2.9 (CH<sub>3</sub>N), 2.9–2.55 (CH<sub>2</sub>O GMA), 2.55–2.10 (CH<sub>2</sub> POxMA), 2.0–1.38 (CH<sub>2</sub> methacrylate), 1.36–0.95 (CH<sub>3</sub> POxMA), 0.95–0.6 (CH<sub>3</sub> methacrylate); SEC (THF, PS standard):  $M_n$  = 21 400 g mol<sup>-1</sup>,  $\delta$  = 1.18.

**Post-Polymerization Modification of PEtOxMA<sub>GMA</sub>:** PEtOxMA (100 mg; 0.003 mmol), PDA (30.6 mg; 0.16 mmol) and triethylamine (15.8 mg; 0.15 mmol) were dissolved in dry DMSO (2 mL) and the solution was stirred at 50 °C overnight. Subsequently, the solvent was removed under reduced pressure. The polymer was re-dissolved in ethanol and dialyzed against Milli-Q water for 3 days. PEtOxMA<sub>PDA</sub> was recovered by freeze-drying. <sup>1</sup>H NMR (400 MHz, CDCl<sub>3</sub>,  $\delta$ ): 8.46, 7.62 (pyridyl), 4.26–3.2 (N-CH<sub>2</sub> POxMA), 3.15–2.85 (CH<sub>3</sub>N), 2.57–2.09 (CH<sub>2</sub> POxMA), 2.0–1.4 (CH<sub>2</sub> methacrylate), 1.4–0.95 (CH<sub>3</sub> POxMA), 0.95–0.6 (CH<sub>3</sub> methacrylate); SEC (THF, PS standard):  $M_n$  = 23 200 g mol<sup>-1</sup>,  $\delta$  = 1.34.

**AF488-labeled Poly(methacrylic acid) (PMA<sub>488</sub>):** To an aqueous PMA solution (30 wt%; 74 mg), 20  $\mu$ L of a DMTMM stock solution (20 mg mL<sup>-1</sup>) was added and stirred for 15 min at room temperature. Subsequently, 20  $\mu$ L of an Alexa Fluor 488 cadaverine stock solution (1 mg mL<sup>-1</sup>, DMSO) was added and stirred overnight at room temperature. The polymer was purified by extensive dialysis against Milli-Q water (3–4 days, with at least two water exchanges per day) and was recovered by freeze-drying.

**Multilayer Assembly on Planar Supports:** Gold-coated 5 MHz AT-cut crystals (Q-Sense AB, Västra, Frölunda, Sweden) were cleaned with piranha solution (7:3 v/v sulfuric acid/hydrogen peroxide) for 20 min followed by extensive rinsing in water, drying with nitrogen, and exposure (20 min) to UV (Bioforce NanoScience, USA). (Caution! Piranha solution is very corrosive. Extreme care should be taken when handling piranha solution, and only small quantities should be prepared.) QCM measurements were conducted using a QCM-D E4 device with four flow cells (Q-Sense AB, Västra, Frölunda, Sweden). All frequency values quoted are for the third overtone. The other overtones measured (fifth and seventh overtones) followed the same trend. According

to the Sauerbrey equation, a frequency change of 1 Hz corresponds to a film mass of  $17.7 \text{ ng cm}^{-2}$  for the 5 MHz QCM crystals used. The temperature was kept constant at  $23^\circ\text{C}$  for the entire deposition process. After initially depositing a layer of PEI ( $1 \text{ g L}^{-1}$  in  $0.5 \text{ M NaCl}$ , 10 min; washed with Milli-Q and subsequently with  $50 \text{ mM NaOAc}$  pH 4), PMA ( $1 \text{ g L}^{-1}$  in  $50 \text{ mM NaOAc}$ , pH 4), and  $\text{P}(\text{EtOxMA}_{\text{SH}})$  ( $1 \text{ g L}^{-1}$  in  $50 \text{ mM NaOAc}$ , pH 4) were sequentially adsorbed to the films until a total number of 14 layers was obtained. After each adsorption step, the films were washed with the same buffer as was used for adsorption ( $0.5 \text{ mL}$ ). For the film degradation studies, four bilayers of  $\text{P}(\text{EtOxMA}_{\text{SH}})$ /PMA were adsorbed onto a PEI/PMA<sub>SH</sub> precursor bilayer. Crosslinking of the films was achieved by incubation with CaT solution. To release the sacrificial PMA, the films were washed with PBS. To allow a comparison of the frequency change, before and after the PMA removal, the films were washed in NaOAc. Degradation was performed by washing the films into PBS again and exposing them to DTT ( $0.1 \text{ M}$ ).

**Multilayer Assembly on Particle Supports:** Prior to use,  $\text{P}(\text{EtOxMA}_{\text{PDA}})$  was dissolved at a concentration of  $100 \text{ g L}^{-1}$  with  $0.5 \text{ M}$  of DTT solution in NaOAc ( $50 \text{ mM}$ , pH 4) for 30 min at  $37^\circ\text{C}$  to expose free thiol groups ( $\text{P}(\text{EtOxMA}_{\text{SH}})$ ). Subsequently, the polymer solution was diluted with NaOAc ( $50 \text{ mM}$ , pH 4) buffer to a concentration of  $1 \text{ g L}^{-1}$ . PMA was directly dissolved in NaOAc ( $50 \text{ mM}$ , pH 4) to a concentration of  $1 \text{ g L}^{-1}$  and pH adjusted.  $100 \mu\text{L}$  of silica particles ( $5 \text{ wt\%}$ ,  $2.59 \mu\text{m}$ -diameter) was washed three times with  $500 \mu\text{L}$  of  $50 \text{ mM NaOAc}$  by centrifugation. To form the multilayers,  $200 \mu\text{L}$  of  $\text{P}(\text{EtOxMA}_{\text{SH}})$  ( $1 \text{ g L}^{-1}$  in  $50 \text{ mM NaOAc}$ , pH 4) was added to the particle suspension for adsorption (12 min) with constant shaking. The particles were then washed via three centrifugation ( $1000 \text{ g}$ , 1 min)/redispersion ( $300 \mu\text{L}$ ) cycles. As the second layer,  $200 \mu\text{L}$  of PMA ( $1 \text{ g L}^{-1}$  in  $50 \text{ mM NaOAc}$ , pH 4) was added to the particle suspension for adsorption (12 min) with constant shaking. The particles were then washed via three centrifugation ( $1000 \text{ g}$ , 1 min)/redispersion ( $300 \mu\text{L}$ ) cycles. This adsorption process was repeated with a further six bilayers of  $\text{P}(\text{EtOxMA}_{\text{SH}})$  and PMA ( $1 \text{ g L}^{-1}$  in  $50 \text{ mM NaOAc}$ , pH 4), followed by one protective capping bilayer of PVPON and PMA ( $1 \text{ g L}^{-1}$  in  $50 \text{ mM NaOAc}$ , pH 4). To follow the assembly of multilayers on particle supports at pH 2, 4, and 5, fluorescently labeled PMA ( $\text{PMA}_{488}$ ) was used for the buildup to monitor the sequential assembly with flow cytometry.  $\text{P}(\text{EtOxMA}_{\text{SH}})$  and  $\text{PMA}_{488}$  were alternately adsorbed onto  $2.59 \mu\text{m}$ -diameter silica particles ( $100 \mu\text{L}$ ), as described above, until 12 layers were deposited (i.e., PMA as the terminating layer) onto the particle supports. After each adsorption step, the core-shell particles were resuspended in  $20 \mu\text{L}$  of NaOAc ( $50 \text{ mM}$ , pH 4) and a  $3 \mu\text{L}$  sample of the particles was taken and analyzed using the flow cytometer.

**Crosslinking of the Multilayers:** After completion of the assembly and extensive washing, the core-shell particles were redispersed in  $400 \mu\text{L}$  of NaOAc ( $50 \text{ mM}$ , pH 4) and shaken at  $37^\circ\text{C}$  overnight in a thermomixer. After washing, the crosslinked core-shell particles were redispersed in  $200 \mu\text{L}$  of NaOAc ( $50 \text{ mM}$ , pH 4). To this suspension,  $400 \mu\text{L}$  of ammonium fluoride ( $8 \text{ M}$ ) and  $200 \mu\text{L}$  of hydrofluoric acid ( $2 \text{ M}$ ) were added for core dissolution, followed by three centrifugation ( $3200 \text{ g}$ , 5 min)/redispersion ( $200 \mu\text{L}$ ) cycles. (Caution! Hydrofluoric acid and ammonium fluoride are very toxic. Extreme care should be taken when handling these solutions, and only small quantities should be prepared.)

**Labeling of the Capsules:** The crosslinked capsules were washed into PBS to remove sacrificial/capping PVPON and PMA layers. The  $\text{P}(\text{EtOxMA}_{\text{SH}})$  capsules were resuspended in  $400 \mu\text{L}$  PBS and  $3 \mu\text{L}$  AF488<sub>mal</sub> ( $1 \text{ g L}^{-1}$ ) was added. After 2 h of constant shaking, the labeled capsules were washed extensively in PBS to remove excess dye.

**Fouling Studies:**  $\text{P}(\text{EtOxMA}_{\text{SH}})$ ,  $\text{PMA}_{\text{SH}}$ ,  $\text{PDPA}_{\text{Alk}}$  and  $\text{P}(\text{EtOxAlk})$  films (5 bilayers) were assembled on QCM electrodes. Details for the synthesis as well as LbL procedures can be found elsewhere:  $\text{P}(\text{EtOxAlk})$ ,<sup>[34]</sup>  $\text{PDPA}_{\text{Alk}}$ ,<sup>[20]</sup>  $\text{PMA}_{\text{SH}}$ .<sup>[45]</sup> For the  $\text{P}(\text{EtOxMA}_{\text{SH}})$  and  $\text{PMA}_{\text{SH}}$  films, a PEI/PMA<sub>SH</sub> precursor bilayer was applied, whereas the alkyne systems had a PEI/PMA<sub>Alk</sub> precursor bilayer. Heating to  $40^\circ\text{C}$ , and incubation with a nondegradable bisazide linker ( $1 \text{ g L}^{-1}$ ), sodium ascorbate ( $4.4 \text{ g L}^{-1}$ ), and copper(II) sulfate ( $1.75 \text{ g L}^{-1}$ ), were used to crosslink the  $\text{P}(\text{EtOxMA}_{\text{SH}})$ /PMA<sub>SH</sub> and  $\text{PDPA}_{\text{Alk}}$ /PMA<sub>SH</sub> films, respectively. After

PMA removal, the films were washed into PBS and incubated in human serum (undiluted) at  $37^\circ\text{C}$  for 45 min. Subsequently, the films were washed with PBS to remove the non-adsorbed serum proteins.

**Intracellular Degradation Studies:** Degradable and nondegradable (control)  $\text{P}(\text{EtOxMA}_{\text{SH}})$  capsules were assembled by crosslinking the thiol pendants upon exposure to heat ( $37^\circ\text{C}$ , overnight) and using a bismaleimide crosslinker, respectively. The degradable and nondegradable capsules were respectively labeled using AF488<sub>mal</sub> (green) and AF647<sub>mal</sub> (red). Both capsules were incubated with JAWS II cells ( $37^\circ\text{C}$ , 5%  $\text{CO}_2$ ) at approximately a 10:1 capsule-to-cell ratio. After 24 h incubation, cells were imaged live using a deconvolution microscope (DeltaVision, Applied Precision,  $60\times 1.42 \text{ NA}$  oil objective) at physiological conditions ( $37^\circ\text{C}$ , 5%  $\text{CO}_2$ ).

**Cell Viability Studies:** JAWS II cells were cultured in a complete media (80% MEM alpha, 20% FBS, and  $2.5 \mu\text{L GM-CSF}$ ) at  $37^\circ\text{C}$ , 5%  $\text{CO}_2$ . Briefly, JAWS II cells were seeded at 5000 cells per well in 96-well plates and incubated with  $\text{P}(\text{EtOxMA}_{\text{SH}})$  capsules at various capsule-to-cell ratios (1:1, 10:1, 50:1, 100:1, and 200:1) in  $200 \mu\text{L}$  of complete media. After 48 h incubation, the complete media was aspirated and replaced with XTT assay solution ( $0.91 \text{ g L}^{-1}$  XTT, 1.8% v/v DMSO, and  $0.14 \text{ g L}^{-1}$  PMS) for 5 h. The absorbance at  $450 \text{ nm}$  was then measured using an Infinite M200 microplate reader (Tecan, Switzerland).

## Supporting Information

Supporting Information is available from the Wiley Online Library or from the author.

## Acknowledgements

K.K. is grateful to the Alexander von Humboldt Foundation (Feodor-Lynen fellowship) for financial support. F.C. acknowledges the Australian Research Council for funding under the Australian Laureate Fellowship scheme (FL1201100030). Marta Redrado Notivoli (Nanomaterials Characterisation Node of the Materials Characterisation and Fabrication Platform, The University of Melbourne) is thanked for assistance with the AFM measurements.

Received: April 30, 2014

Revised: June 6, 2014

Published online: August 13, 2014

- [1] T. M. Allen, P. R. Cullis, *Science* **2004**, 303, 1818.
- [2] K. E. Uhrich, S. M. Cannizzaro, R. S. Langer, K. M. Shakesheff, *Chem. Rev.* **1999**, 99, 3181.
- [3] R. P. Brinkhuis, F. P. J. T. Rutjes, J. C. M. van Hest, *Polym. Chem.* **2011**, 2, 1449.
- [4] L. L. del Mercato, P. Rivera-Gil, A. Z. Abbasi, M. Ochs, C. Ganas, I. Zins, C. Sonnichsen, W. J. Parak, *Nanoscale* **2010**, 2, 458.
- [5] A. P. Esser-Kahn, S. A. Odom, N. R. Sottos, S. R. White, J. S. Moore, *Macromolecules* **2011**, 44, 5539.
- [6] A. P. R. Johnston, G. K. Such, F. Caruso, *Angew. Chem. Int. Ed.* **2010**, 49, 2664.
- [7] J. Cui, M. P. van Koeven, M. Muellner, K. Kempe, F. Caruso, *Adv. Colloid Interface Sci.* **2014**, 207, 14.
- [8] A. L. Becker, A. P. R. Johnston, F. Caruso, *Small* **2010**, 6, 1836.
- [9] S. De Koker, R. Hoogenboom, B. G. De Geest, *Chem. Soc. Rev.* **2012**, 41, 2867.
- [10] G. Decher, *Science* **1997**, 277, 1232.
- [11] F. Caruso, R. A. Caruso, H. Mohwald, *Science* **1998**, 282, 1111.
- [12] G. K. Such, A. P. R. Johnston, F. Caruso, *Chem. Soc. Rev.* **2011**, 40, 19.

- [13] C. S. Peyratout, L. Dahne, *Angew. Chem. Int. Ed.* **2004**, *43*, 3762.
- [14] C. J. Ochs, G. K. Such, Y. Yan, M. P. van Koeverden, F. Caruso, *ACS Nano* **2010**, *4*, 1653.
- [15] C. R. Kinnane, G. K. Such, G. Antequera-Garcia, Y. Yan, S. J. Dodds, L. M. Liz-Marzan, F. Caruso, *Biomacromolecules* **2009**, *10*, 2839.
- [16] M. Dierendonck, K. Fierens, R. De Rycke, L. Lybaert, S. Maji, Z. Zhang, Q. Zhang, R. Hoogenboom, B. N. Lambrecht, J. Grooten, J. P. Remon, S. De Koker, B. G. De Geest, *Adv. Funct. Mater.* **2014**, DOI: 10.1002/adfm.201400763.
- [17] M. K. M. Leung, G. K. Such, A. P. R. Johnston, D. P. Biswas, Z. Y. Zhu, Y. Yan, J. F. Lutz, F. Caruso, *Small* **2011**, *7*, 1075.
- [18] I. Erel, H. Schlaad, A. L. Demirel, *J. Colloid Interface Sci.* **2011**, *361*, 477.
- [19] A. B. D. F. Antunes, M. Dierendonck, G. Vancoillie, J. P. Remon, R. Hoogenboom, B. G. De Geest, *Chem. Commun.* **2013**, *49*, 9663.
- [20] K. Liang, G. K. Such, Z. Y. Zhu, Y. Yan, H. Lomas, F. Caruso, *Adv. Mater.* **2011**, *23*, H273.
- [21] A. N. Zelikin, J. F. Quinn, F. Caruso, *Biomacromolecules* **2006**, *7*, 27.
- [22] R. Cheng, F. Feng, F. H. Meng, C. Deng, J. Feijen, Z. Y. Zhong, *J. Control. Release* **2011**, *152*, 2.
- [23] M. Huo, J. Yuan, L. Tao, Y. Wei, *Polym. Chem.* **2014**, *5*, 1519.
- [24] N. Ma, Y. Li, H. Xu, Z. Wang, X. Zhang, *J. Am. Chem. Soc.* **2010**, *132*, 442.
- [25] H. Xu, W. Cao, X. Zhang, *Acc. Chem. Res.* **2013**, *46*, 1647.
- [26] H. Ren, Y. Wu, Y. Li, W. Cao, Z. Sun, H. Xu, X. Zhang, *Small* **2013**, *9*, 3981.
- [27] G. Y. Wu, Y. Z. Fang, S. Yang, J. R. Lupton, N. D. Turner, *J. Nutr.* **2004**, *134*, 489.
- [28] F. H. Meng, W. E. Hennink, Z. Zhong, *Biomaterials* **2009**, *30*, 2180.
- [29] A. N. Zelikin, Q. Li, F. Caruso, *Chem. Mater.* **2008**, *20*, 2655.
- [30] A. Sexton, P. G. Whitney, S. F. Chong, A. N. Zelikin, A. P. R. Johnston, R. De Rose, A. G. Brooks, F. Caruso, S. J. Kent, *ACS Nano* **2009**, *3*, 3391.
- [31] Y. Yan, A. P. R. Johnston, S. J. Dodds, M. M. J. Kamphuis, C. Ferguson, R. G. Parton, E. C. Nice, J. K. Heath, F. Caruso, *ACS Nano* **2010**, *4*, 2928.
- [32] K. Liang, G. K. Such, Z. Y. Zhu, S. J. Dodds, A. P. R. Johnston, J. W. Cui, H. Ejima, F. Caruso, *ACS Nano* **2012**, *6*, 10186.
- [33] S. F. Chen, L. Y. Li, C. Zhao, J. Zheng, *Polymer* **2010**, *51*, 5283.
- [34] K. Kempe, S. L. Ng, K. F. Noi, M. Müllner, S. T. Gunawan, F. Caruso, *ACS Macro Lett.* **2013**, *2*, 1069.
- [35] R. Hoogenboom, *Angew. Chem. Int. Ed.* **2009**, *48*, 7978.
- [36] A. Makino, S. Kobayashi, *J. Polym. Sci., Part A: Polym. Chem.* **2010**, *48*, 1251.
- [37] B. Guillermin, S. Monge, V. Lapinte, J. J. Robin, *Macromol. Rapid Commun.* **2012**, *33*, 1600.
- [38] C. Weber, C. R. Becer, R. Hoogenboom, U. S. Schubert, *Macromolecules* **2009**, *42*, 2965.
- [39] J. Huotari, A. Helenius, *EMBO J.* **2011**, *30*, 3481.
- [40] I. Banerjee, R. C. Pangule, R. S. Kane, *Adv. Mater.* **2011**, *23*, 690.
- [41] L. Tauhardt, K. Kempe, M. Gottschaldt, U. S. Schubert, *Chem. Soc. Rev.* **2013**, *42*, 7998.
- [42] G. Sauerbrey, *Z. Phys.* **1959**, *155*, 206.
- [43] E. F. Crownover, A. J. Convertine, P. S. Stayton, *Polym. Chem.* **2011**, *2*, 1499.
- [44] C. Weber, C. R. Becer, A. Baumgaertel, R. Hoogenboom, U. S. Schubert, *Des. Monomers Polym.* **2009**, *12*, 149.
- [45] A. L. Becker, A. N. Zelikin, A. P. R. Johnston, F. Caruso, *Langmuir* **2009**, *25*, 14079.